

# Automated image analysis in large-scale cellular electron microscopy: A literature survey

Anusha Aswath<sup>a,b,\*</sup>, Ahmad Alsahaf<sup>b</sup>, Ben N. G. Giepmans<sup>b</sup>, George Azzopardi<sup>a</sup>

<sup>a</sup>*Bernoulli Institute of Mathematics, Computer Science and Artificial Intelligence, University Groningen, Groningen, The Netherlands*

<sup>b</sup>*Dept. Biomedical Sciences of Cells and Systems, University Groningen, University Medical Center Groningen, Groningen, The Netherlands*

---

## Abstract

Large-scale electron microscopy (EM) datasets generated using (semi-) automated microscopes are becoming the standard in EM. Given the vast amounts of data, manual analysis of all data is not feasible, thus automated analysis is crucial. The main challenges in automated analysis include the annotation that is needed to analyse and interpret biomedical images, coupled with achieving high-throughput. Here, we review the current state-of-the-art of automated computer techniques and major challenges for the analysis of structures in cellular EM. The advanced computer vision, deep learning and software tools that have been developed in the last five years for automatic biomedical image analysis are discussed with respect to annotation, segmentation and scalability for EM data. Integration of automatic image acquisition and analysis will allow for high-throughput analysis of millimeter-range datasets with nanometer resolution.

*Keywords:* Electron microscopy, segmentation, supervised, unsupervised, machine learning, deep learning, AI

---

## 1. Large-scale cellular EM

Electron microscopy (EM) is widely used in life sciences to study tissues, cells, subcellular components and (macro) molecular complexes at nanometer scale. Two-dimensional (2D) EM aids in diagnosis of diseases, but routinely it still depends upon biased snapshots of areas of interest. Automated pipelines for collection, stitching and open access publishing of 2D EM have been pioneered for both transmission EM (TEM) images (Faas et al., 2012) as well as scanning TEM (STEM) (Sokol et al., 2015) for acquisition of areas up to 1mm<sup>2</sup> at nanometer-range resolution, Table. 1. Nowadays, imaging of large areas at

---

\*Corresponding author:

Email address: [a.aswath@rug.nl](mailto:a.aswath@rug.nl) (Anusha Aswath)

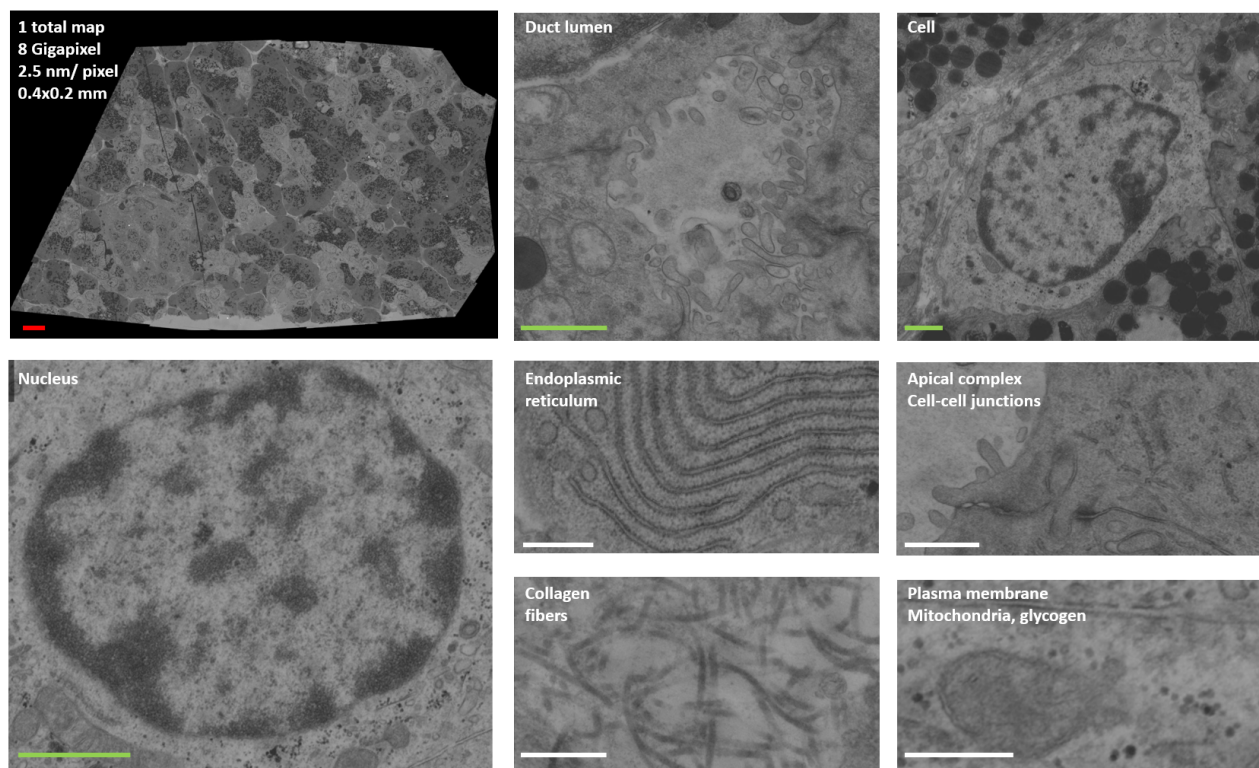


Figure 1: Typical large-scale EM allows to analyze tissue at a high resolution. Overview and snapshots of several cellular, subcellular and macromolecular structures of which up to a million can be present per dataset (de Boer et al., 2020). Bars: red  $10\mu\text{m}$ ; green  $1\mu\text{m}$ ; white  $0.5\mu\text{m}$ . Full access to digital zoomable data at full resolution is via <http://www.nanotomym.org>.

high resolution is entering the field as a routine method and is provided by most EM manufacturers. This we term nanotomym, for nano-anatomy (Ravelli et al., 2013; de Boer et al., 2020; Dittmayer et al., 2021). The large-scale images allow for open access world-wide data sharing; see [nanotomym.org](http://nanotomym.org)<sup>1</sup> for more than 40 published studies and the accessible nanotomym data.

A typical nanotomym dataset has a size of 5-25GB at 2.5nm pixel size. Nanotomym allows scientists to pan and zoom through different tissues or cellular structures in a Google Earth-like manner (Fig. 1). Large-scale 2D EM provides unbiased data recording to discover events such as pathogenesis of diseases at the supra-cellular level for morphological changes. Moreover, nanotomym allows for the quantification of subcellular hallmarks. With state-of-the-art 2D EM tech-

<sup>1</sup>[www.nanotomym.org](http://www.nanotomym.org)

<sup>2</sup><https://myscope.training/>

Table 1: Major large-scale EM techniques. Note that the biomaterial for the techniques below is stained with heavy metals to generate contrast. For further information see the MyScope website<sup>2</sup> and the papers reviewed by Peddie and Collinson (2014) and Titze and Genoud (2016).

2D EM	Methodology
Transmission Electron Microscopy (TEM)	A widefield electron beam illuminates an ultra-thin specimen and transmitted electrons are detected at the other side of the sample. The structure that is electron dense appears dark and others appear lighter depending on their (lack of) scattering.
Scanning Electron Microscopy (SEM)	The raster scanning beam interacts with the material and can result in back scattering or formation of secondary electrons. Their intensity reveals sample information.
Scanning Transmission Electron Microscopy (STEM)	SEM on ultrathin sections and using a detector for the transmitted electrons.
3D EM	
Serial section TEM (ssTEM) or SEM (ssSEM)	Volume EM technique for examining 3D ultrastructure by scanning adjacent ultrathin (typical 60-80 nm) sections using TEM or SEM, respectively.
Serial Block-face scanning EM (SB SEM)	The block face is scanned followed by removal of the top layer by a diamond knife (typical 20-60 nm) and the newly exposed block face is scanned. This can be repeated thousands of times.
Focused Ion Beam SEM (FIB-SEM)	Block face imaging as above, but sections are repeatedly removed by a focused ion beam that has higher precision than a knife (typically down to 4 nm) suitable for smaller volumes.

nology, such as multibeam scanning EM (Eberle et al., 2015; Ren and Kruit, 2016), up to 100 times faster acquisition and higher throughput allows for imaging of tissue-wide sections in the range of hours instead of days. For a side by side example of single beam versus multibeam nanotomy, see de Boer and Giepmans (2021). Given the automated and faster image acquisition in 2D EM a data avalanche (petabyte-range per microscope/month) will soon be a reality.

Automated large-scale three-dimensional (3D) or volume EM (vEM), which creates a stack of images, is also booming as reviewed by Peddie and Collinson (2014); Titze and Genoud (2016); Peddie et al. (2022) (Table. 1). Examples include whole-cell volume reconstruction of up to 35 cellular organelle classes (Heinrich et al., 2021). The data acquisition time is not the bottleneck anymore, but data analysis is. Note that one person needed two weeks to manually label a fraction ( $1\mu m^3$ ) of the imaged volume. The whole cell could take 60 person years. Hence, the urgent need for automatic image analysis.

Semantic segmentation of EM images is the automatic process of mapping each pixel to known or newly discovered classes of subcellular structures. The challenges of automatic segmentation of EM images are due to the rendering in one color channel (grayscale) of subcellular structures with different sizes, shapes

and heterogeneous appearances, further surrounded by complicated structures. 2D EM datasets only have neighbouring ( $X/Y$  axes) context as reference for structural analysis. The vEM datasets leverage knowledge from adjacent sections ( $Z$ -axis) that share high resemblance, and therefore aids in better reconstruction of the volume. Additionally, large-scale 2D EM images are more spatially distributed across cells than traditional EM micrographes of a selected region or vEM that occupy a smaller spatial area, despite both large-scale 2D EM and vEM containing gigabytes of information. It requires global image processing without losing coherent information.

Here, we review automated methods for large scale EM image segmentation and analysis.

## 2. Deep learning and segmentation

Deep learning has become the state-of-the-art methodology for many computer vision tasks, including segmentation. This has been a paradigm shift when compared to traditional segmentation methods, which were generally performed using machine learning classifiers such as Adaboost, Random forests, and Support Vector Machines (SVMs), which required domain-oriented, hand-crafted features as inputs (Table 2). The introduction of Deep Neural Networks (DNNs) has enabled automatic extraction of hierarchical representations from raw image data (LeCun et al., 2015). Convolutional Neural Networks (CNN) have significantly advanced image-related tasks such as classification, detection, and segmentation with end-to-end learning from feature extraction to prediction.

A typical CNN consists of convolutional filters or weight sharing filter banks in each layer of the neural network. Convolutional filters are linear functions that are used for low-level basic operations, such as blurring and edge detection. A 2D convolutional filter uses a 2D matrix, referred to as a kernel, centered on a local region in a given image and applies a linear operation between the kernel coefficients and the respective pixel values in the local region concerned. The resulting scalar value is the response of the filter to the considered region. The filter is then slid across the whole image to compute the responses at every location. All responses form what is known as a response or a feature map which has the same size as the input image if the sliding is done one pixel at a time. 3D filters operate in a similar way but use 3D kernels and are applied to 3D volumes of vEM images. In a CNN, the filters allow for weight sharing throughout the image capturing structured data using translational and rotational invariance (Krizhevsky et al., 2012; Yamashita et al., 2018). The spatial extent of the connectivity of a filter with local pixels is called the receptive field or the kernel size. The response maps obtained by such filters are then processed by a non-linear activation function, before being downsampled by a pooling unit in order to learn abstract representations (LeCun et al., 2015). Finally, the response maps are fed to a fully connected layer which determines a label for the given image.



Table 2: Definitions of common terms used in the literature of machine/deep learning frameworks.

	Terms	Definition	Notes
Descriptors	Handcrafted	Functions that are implemented using domain expertise for the extraction of features.	Examples include the Canny edge detector, Harris corner detector, and more sophisticated ones, such as HOG, LBP, SIFT, and SURF. (Dalal and Triggs, 2005; Wang and He, 1990; Lowe, 2004)
	Trainable	Functions that learn features from given training sets. Such descriptors can be contour-, color- or texture-based.	The trainable COSFIRE approach is an example of contour- and color-based trainable descriptor (Azzopardi and Petkov, 2012; Gecer et al., 2017).
Classifiers	Linear	A model that separates a given feature space with a linear boundary. In a 2D space the model is simply a line, while a plane and hyperplanes are used for 3D and higher dimensional spaces.	Logistic regression and Support Vector Machines (SVMs) are examples of linear classifiers. The latter learns a linear classifier after transforming the input features to a higher dimensional space. (Dreiseitl and Ohno-Machado, 2002; Boser et al., 1992)
	Non-linear	A model that learns a non-linear function to separate classes. The degree of non-linearity is arbitrary. Generalization error tends to increase with increasing non-linearity. Regularization is a technique used to keep a good tradeoff between non-linearity and generalization.	Neural networks (NNs), such as deep NNs (DNNs), fully connected NNs (FCNNs) and convolutional NNs (CNNs), are end-to-end models that learn features from the training set and a non-linear function that maps the input to output via the learned features (Glorot and Bengio, 2010)
Meta-learners	Weak and Strong learners	A weak learner is a model that performs just better than random guessing, while a strong learner is a model that achieves high performance.	Decision trees are data structures that define classes. Decision trees with very few and with many layers can be considered as weak and strong learners, respectively (Drucker and Cortes, 1995)
	Ensemble modeling	The combination of outcomes of multiple learners to achieve better predictive performance while reducing the risk of overfitting.	<b>Boosting</b> aggregates outputs of different weak learners in an iterative manner. <b>Bagging</b> trains weak learners concurrently on subsets of independent and identically distributed data (IID) sampled with replacement. <b>Random forest</b> ; a group of decision trees that learn with bagging and random feature sampling (Breiman, 2001).
Deep Learning	Deep neural networks (DNNs)	Deep learning is a subset of machine learning, that uses a neural network with three or more layers. Such networks automatically extract input features from unstructured data unlike conventional machine learning that use hand-crafted features.	Popular deep neural networks are Convolutional neural networks (CNNs), Recurrent neural networks (RNNs), Long-short Term memory (LSTMs), and Autoencoders (Hochreiter and Schmidhuber, 1997; Masci et al., 2011).
	Convolutional Neural Networks (CNN)	Convolutional DNNs with convolutional layers. Convolutional layers consist of nodes that apply linear filters by scanning a given image in overlapping blocks of pixels to extract features. Besides convolutions each layer includes a nonlinear activation function followed by down sampling.	Examples include <b>AlexNet</b> (Krizhevsky et al., 2012) an early deep CNN designed to classify a thousand categories of images (ImageNet). <b>VGG</b> (Simonyan and Zisserman, 2014) reduced the number of parameters by using smaller filters multiple times between layers. Residual Neural network ( <b>ResNet</b> ) (He et al., 2016) trains deeper networks efficiently using residual blocks that connect outputs of stacked layers to the block’s input layer with identity skip connections.
Challenges with DNNs	Vanishing gradient	Occurs when the partial derivatives of the loss function (error between the ground truth and prediction) in a learning algorithm (e.g. gradient descent) become very close to zero. The learning algorithm is unable to back-propagate useful gradient information.	Caused by activation functions (e.g. sigmoid) that map a large input space to the limited range [0,1], leading to very small derivatives even when the input change is large. Using activation functions (e.g. ReLU) that avoid small derivatives is an effective way to address the vanishing gradient problem (Krizhevsky et al., 2012).
	Degradation in DNNs	Deeper additional layers that provide the network power to calculate a more complex function without increasing the training set may lead to a performance saturation and eventually degradation.	ResNets allow for uninterrupted flow of information from previous layers to subsequent ones, realising a complex function with less parameters and hence less risk of both degradation and vanishing gradients (He et al., 2016)

Progress in the development of CNNs has led to a plethora of applications including the automatic analysis of medical images. The CNN designed by Ciresan et al. (2012), for instance, was used for the segmentation of neuronal membranes in stacks of EM images. The images were segmented by predicting the label of each local region or patch covered by a convolutional filter in a sliding window approach. Despite the method’s success - winning the 2012 ISBI<sup>3</sup> EM segmentation challenge - the method has two major limitations. First, the sliding window approach is slow as it suffers from redundancy due to the processing of large overlaps between adjacent patches. Second, there is always a trade-off between the size of the patches (context) and full-resolution prediction. It turns out that localisation ability decreases with an increasing context due to downsampling by the many max pooling layers. Improvements in the semantic segmentation of EM images continued with the development of the Fully Convolutional Network (FCN) (Long et al., 2015). FCN allows for variable sized images as input by replacing the fully connected layers of a standard CNN with fully convolutional maps (Fig. 2). Now, the spatial maps in the last layer of an FCN correspond to certain local patches or pixels of an input image depending on the network depth.

Encoder-decoder architectures of the FCN type have been catalysts in providing better localization and use of larger context. The decoder also captures multi-scale features using skip connections to fuse feature maps from shallow layers, providing larger context. Skip connections bypass some of the neural network layers and take the output of one layer as the input to the subsequent ones. As a result, an alternative and shorter path is provided for backpropagating the error of the loss function, which also contributes in avoiding the vanishing gradient and the degradation problems in deep networks (Table 2). In principle, skip connections allow for a better upsampling in higher layers. For instance, the symmetric U-Net architecture transfers full feature maps from the encoder to the decoder paths, achieving the best segmentation results of neuronal membranes in EM images in the ISBI 2015 challenge (Ronneberger et al., 2015). SegNet was proposed to transfer only the pooling indices between the encoder and decoder paths to reduce the load on memory (Badrinarayanan et al., 2017). Nevertheless, U-Net captures more complex information from the stored encoder layer outputs concatenated using skip connections for upsampling and thus outperforms SegNet in terms of accuracy.

The concept of convolutional output layers in FCNs enables the conversion of popular DNNs, such as AlexNet, VGGNet, ResNet and GoogleNet (Inception-v1) (Krizhevsky et al., 2012; Simonyan and Zisserman, 2014; He et al., 2016; Szegedy et al., 2015), into encoder-decoder architectures for semantic segmentation. DNNs are universal approximators that can realise a complex function with even two layers of the network. Shallow neural networks with a few layers are not adequate to learn robust models due to overfitting. Deeper networks with small receptive fields, such as VGG-16 and AlexNet, became popular for

---

<sup>3</sup>IEEE International Symposium on Biomedical Imaging.

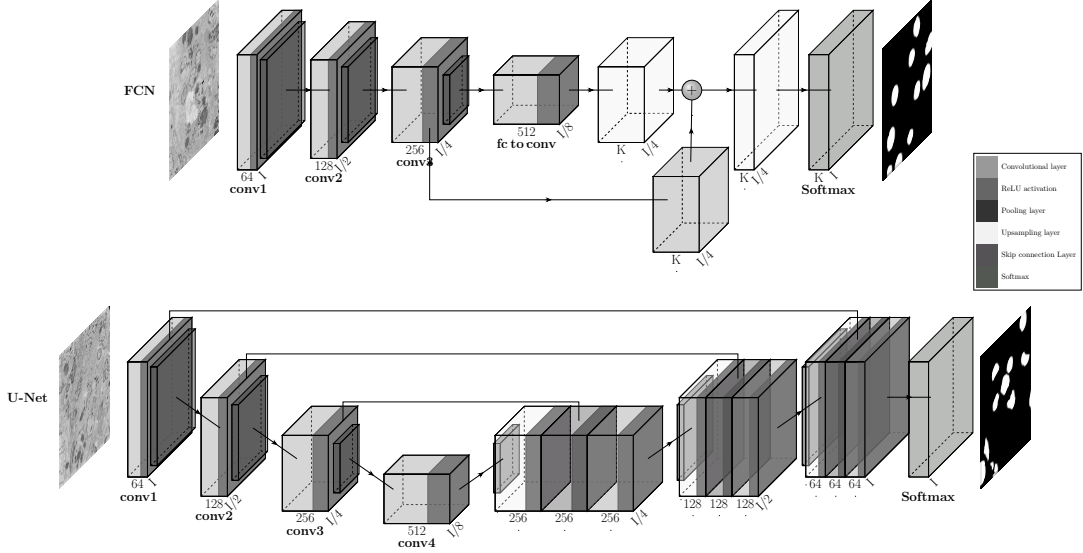


Figure 2: Encoder-decoder networks for FCN and U-Net. Each of the first four convolutional layers in the encoder are followed by the nonlinear activation function ReLU and max pooling. The last layer uses a softmax function to assign a probability class score to each pixel. The FCN decoder includes an upsampling component that is linearly combined with the low-level feature maps in the third convolutional layer of the encoder. The sizes of these feature maps are 4 times less than the size of the input image  $I$  (denoted by  $I/4$ ). Finally, there is a direct upsampling from  $I/4$  to the original size of  $I$  followed by softmax for classification. The symmetrical U-Net architecture shares the features maps in the encoder with the decoder path together with skip connections.

image classification due to their generalization ability. DNNs have a large number of parameters to learn using the loss function (or error) that quantifies the penalty of the predicted values with respect to the desired ones. The addition of layers to make an architecture deeper brings other scientific challenges, such as the vanishing gradient and network degradation (Table. 2). Methods to address these challenges with training deeper networks include different strategies in initializing network parameters (Glorot and Bengio, 2010), training networks in multiple stages (Simonyan and Zisserman, 2014), and using companion loss functions or auxiliary supervision in the middle layers (Szegedy et al., 2015). The most recent and important networks in computer vision are called the Residual Neural Networks or ResNet that overcame the vanishing gradient and the degradation issues simultaneously (Table. 2).

Spatial pyramid pooling and dilated (or atrous) convolutions were introduced in the DeepLab family of segmentation architectures for the purpose of larger context capture. DeepLab models addressed the challenges of achieving robustness for different scales of classes and considering larger context without increasing computational complexity (Chen et al., 2014, 2017a,b, 2018). Moreover, multi-scale context aggregation using the Pyramid Scene Parsing Network

(PSP-Net) or spatial attention using the attention U-Net have also gained popularity for their ability to capture larger context (Zhao et al., 2017; Oktay et al., 2018). The ability to deal with varying scales while capturing more context is particularly important in EM analysis where the neighbourhood of a structure may have an impact in determining a precise delineation.

### 3. Literature search

The following search query was used in both Pubmed and Web of Science on words in titles (TI) only, restricted to 2017-2021: TI=((electron microscopy OR EM) AND (segmentation OR supervised OR unsupervised OR self-supervised)) NOT cryo. Cryo-EM (Kucukelbir et al., 2014) was excluded because it involves molecule datasets as opposed to cellular EM. Results from the query that are beyond our scope were excluded. A detailed review of the resulting 28 papers (Table 3) is given in terms of the data annotation and studied structures, the segmentation approaches, and computational scalability.

### 4. Data, anatomical structures and annotation

Early examples of automated segmentation include the reconstruction of brain tissues for connectomics, which is the map of neuronal cell bodies and their connections, the synapses. The pioneer work on automated neuronal membrane segmentation by Ciresan et al. (2012) showed the success of neural networks on EM images in the ISBI 2012 challenge. This has motivated more research activity in this direction, resulting in key segmentation architectures such as U-Net (Ronneberger et al., 2015). Properties of the most commonly used datasets are shown in Table 4.

Large-scale connectome datasets mostly focused on sub-cellular components related to brain cells such as synapses, pre- and post-synaptic sites, axons and mitochondria (Takemura et al., 2015; Kasthuri et al., 2015). The open organelle project provides free access to high resolution 3D EM datasets and their segmentations for analysing intracellular sub-structures and organelles <sup>4</sup>. With the challenge to automatically reconstruct tissues at cellular level, several organelles besides mitochondria, namely nucleus, plasma membrane, endoplasmic reticulum, nuclear envelope, vesicles, lysosomes, endosomes and microtubules have now become the focus in open-source datasets (Heinrich et al., 2021).

Detailed annotation of large-scale EM images is required for automatic image segmentation and analysis of structures. Three approaches of annotations are considered: 1) *human annotators*; 2) *software tools for biologists*; and 3) *specialized microscopy imaging modalities*.

---

<sup>4</sup><https://www.openorganelle.org/>

Table 3: Survey papers. Abbreviations used - S (Supervised), UN (Unsupervised), SS (Semi-supervised), F (FIB-SEM), SS (Serial section), SB (SB-SEM).

Method	Type	Dataset		EM type				Structures	Study
		2D	3D	F	SS	SB	TEM		
Residual Deconvolutional Network (RDN)	S	✓	-	✓	✓	-	-	Membranes	Fakhry et al. (2016)
DeepEM3D	S	-	✓	-	✓	-	-	Membranes	Zeng et al. (2017)
Feature selection and boosting	S	-	✓	-	-	✓	-	Mitochondria, synapses, membranes	Cetina et al. (2018)
Pre-trained networks	S	-	✓	✓	-	✓	-	Neurophil, axons	Drawitsch et al. (2018)
2D Convolutional Neural Network (CNN)	S	✓	-	✓	-	-	-	Mitochondria	Oztel et al. (2018)
3D Residual FCN	S	-	✓	✓	✓	-	-	Mitochondria	Xiao et al. (2018)
Two-stream U-Net	UN	-	✓	✓	✓	-	-	Mitochondria, synapses	Bermúdez-Chacón et al. (2019)
Random forest	S	✓	-	-	-	-	✓	Glomular basement membrane	Cao et al. (2019)
Fully Convolutional Network (FCN)	S	✓	-	✓	-	-	-	Mitochondria	Dietlmeier et al. (2019)
Fully Residual U-Net (FRU-Net)	S	✓	-	✓	-	-	-	Membranes	Gómez-de Mariscal et al. (2019)
3D Convolutional Neural Network (CNN)	S	✓	✓	✓	-	✓	-	Cells, mitochondria, membranes	Guay et al. (2019)
Residual Neural Network (ResNet)	S	✓	-	-	✓	-	-	Neural cell body, cell nucleus	Jiang et al. (2019)
Morphological operators/superpixels	UN	-	✓	✓	-	✓	-	Mitochondria, membranes	Karabağ et al. (2019)
Random forest	S	✓	✓	✓	✓	-	-	Mitochondria	Peng and Yuan (2019)
U-Net, ResNet, HighwayNet, DenseNet	S	-	✓	✓	-	-	-	Membranes	Urakubo et al. (2019)
DenseUNet	S	✓	-	✓	-	-	-	Mitochondria	Cao et al. (2020)
Fully residual CNN (FR-CNN)	S	✓	-	✓	-	-	-	Membranes	He et al. (2020)
HighRes3DZMNet	S	-	✓	✓	-	-	-	Mitochondria, endolysosomes	Mekuč et al. (2020)
U-Net, autoencoder	UN	✓	✓	✓	✓	-	-	Mitochondria	Peng et al. (2020)
DeepACSON	S	-	✓	✓	-	-	-	Axons	Abdollahzadeh et al. (2021)
2D-3D hybrid network	S	✓	✓	-	-	✓	-	Cells, granules, mitochondria	Guay et al. (2021a)
3D U-Net	S	-	✓	✓	-	-	-	Up to 35 sub-cellular structures	Heinrich et al. (2021)
CDeep3EM, EM-Net, PReLU-Net, ResNet	S	✓	-	✓	-	-	-	Mitochondria	Khadangi et al. (2021b)
Hierarchical encoder-decoder (HED-Net)	S	✓	✓	✓	✓	-	-	Mitochondria	Luo et al. (2021)
Generative adversarial network (GAN)	UN	✓	-	-	-	-	✓	Cytoplasmic caspids	Shaga Devan et al. (2021)
Annotation-crowd-sourcing, ‘Etch a Cell’	S	-	✓	-	-	✓	-	ER, mitochondria, nucleus	Spiers et al. (2021)
U-Net	SS	-	✓	✓	-	-	-	Membranes	Takaya et al. (2021)
Hierarchical view ensemble (HIVE) Net	S	✓	✓	✓	✓	-	-	Axons, nuclei, mitochondria	Yuan et al. (2021)

Table 4: Commonly re-used 3D EM datasets for image analysis improvement.

Acquisition	Dataset	Region	Imaged tissue parameters (x,y,z)			Reference
			Volume ( $\mu m$ )	Pixels	Pixel size ( $nm$ )	
ssTEM	ISBI 2012 / Drosophila I VNC	Nervous cord (Drosophila)	$2 \times 2 \times 1.5$	$512 \times 512 \times 30$	$4 \times 4 \times 50$	Ciresan et al. (2012)
ssSEM	ISBI 2013 / SNEMI3D	Cerebral cortex (Mouse)	$6 \times 6 \times 6$	$1024 \times 1024 \times 100$	$6 \times 6 \times 30$	Arganda- Carreras et al. (2013)
ssSEM	Kasthuri dataset	Neocortex (Mouse)	$10^3 \times 10^3 \times 130$	$1024 \times 1024 \times 2000$	$3 \times 3 \times 30$	Kasthuri et al. (2015)
SB SEM	HeLa cells	Cultured cells (Human)	$1 \times 1 \times 0.2$	$8192 \times 8192 \times 518$	$10 \times 10 \times 50$	Iudin et al. (2016)
FIB-SEM	EPFL Mouse Hippocampus	CA1 Hippocampus (Mouse)	$5 \times 5 \times 5$	$2048 \times 1536 \times 1065$	$5 \times 5 \times 5$	Lucchi et al. (2013)
FIB-SEM	FIB-25	Optic lobe (Drosophila)	$64 \times 66 \times 81$	$6426 \times 6623 \times 8090$	$10 \times 10 \times 10$	Takemura et al. (2015)

#### 4.1. Human annotators

Human annotation is split into two categories, annotations by one or a few experts, and collaborative annotations by large groups of experts and non-experts, so-called crowd-sourced annotation. Projects such as Etch-a-Cell enable annotation through crowd-sourcing (Spiers et al., 2021) that allows volunteers to participate in large-scale annotation tasks digitally, with the aid of tutorials and other guided workflows. For example, volunteers are invited to annotate certain structures, such as endoplasmic reticulum (ER), mitochondria or nuclei, in order to collect ground truth segmentation labels for supervised machine learning algorithms. As human segmentations can be erroneous due to imprecise delineation of structures or bias, consensus between various volunteer segmentations is often used as the ground truth. Expert annotations are more accurate but require more time and resources. For example, labeling structures in 30 platelets from a small fraction of the imaged samples required 9 months from two human annotators (Guay et al., 2021a). Also, the large scale connectomics project required extensive labelling of ground truth data (Plaza and Funke, 2018), and the proofreading<sup>5</sup> of the ground truth dataset took around 5 years in the work of Takemura et al. (2015).

#### 4.2. Biomedical image analysis software

Biomedical image analysis software applications are black box tools for many users to annotate or proofread EM datasets without having to know the under-

<sup>5</sup>Proofreading refers to the manual correction of segmented (manual or automatic) image data.

lying mechanisms<sup>6</sup>. Large-scale connectome reconstruction prompted the development of various tools for proofreading and analysis of the reconstructed data. All the tools are mostly developed for connectome proofreading and analysis for serial sectioned image stacks and block-face images. Such tools mostly come with 2D viewers and 2D annotations using brush/flood-fill functions with 3D viewers for visualization (Table 5). Generally, the reconstructed or annotated maps are corrected by reading data from external servers. The data storage format in the server and the mechanism of data distribution to the client determine how well the tool can scale for annotation or proofreading of larger volumes.

No single software tool is typically enough for the entire automated image analysis pipeline. UNI-EM bundles several off-the-shelf tools for annotation, segmentation, proofreading or multi-view rendering into a single package (Urakubo et al., 2019). Entire segmentation workflow is included using DOJO, CNN models such as U-Net, ResNet, Highway Net, DenseNet and flood filling networks (Srivastava et al., 2015; Huang et al., 2017; Januszewski et al., 2018) and an additional 3D surface-mesh based renderer. DOJO is a web-based tool for large-scale annotation and proofreading (Haehn et al., 2014). The package also includes monitoring tools such as TensorBoard for performance monitoring (Mané et al., 2015). The user does not need programming skills to perform segmentation.

TrackEM2 is a software tool for optimized manual and semi-automatic reconstruction of neuronal circuits (Xiao et al., 2018; Jiang et al., 2019; Ciresan et al., 2012; Li et al., 2018). A companion tool for TrackEM2 is CATMAID, which is for data storage, management and collaborative annotation of large-scale 3D ssTEM datasets using a client-server model (Saalfeld et al., 2009). However, 3D neurite tracing to the next lateral 2D image plane obtained from a server can be less optimal due to low bandwidth and network latency issues. To overcome this challenge, webKnossos uses a 3D SB SEM dataset storage and transmission in the form of small 3D voxels, as used in Knossos (a standalone data annotation application for connectomics) (Helmstaedter et al., 2011). WebKnossos is a cloud/browser-based 3D annotation tool for large-scale distributed data analysis (Boergens et al., 2017). An example of open-source demo for dense connectome reconstruction using webKnossos is given by Motta et al. (2019). 3D voxel based storage and access is also provided by VAST (Volume Annotation and Segmentation Tool) to handle petabyte range image data. Rich metadata based information can be generated for segmented objects and be grouped or organised in a tree structure for importing. Similar to CATMAID, VAST has a data management framework with specific file format conversion before analysis (Berger et al., 2018). A VAST format compatible dataset is publicly available to annotate the mitochondria dataset by Kasthuri et al. (2015)<sup>7</sup>.

The FlyEM project provides open-source tools which aim to fully reconstruct the neural connectivity of the *Drosophila* fly brain using EM imaging (Scheffer

---

<sup>6</sup><http://www.biii.eu/>

<sup>7</sup>[lichtman.rc.fas.harvard.edu/vast/](http://lichtman.rc.fas.harvard.edu/vast/)

Table 5: Reviewed biomedical image analysis software for manual or semi-automatic image segmentation, annotation and proofreading.

Feature/ Software	Visualization client	Annotation client	Collaborative annotation	Data con- version format	Scalability	Train/Test	Inclusion of custom algorithm
<b>UNI-EM</b>	2D, 3D/DOJO	2D DOJO, 3D Mesh	Web-based	PNG/TIFF	High	DNN	Python script
<b>webKnossos</b>	2D, 3D/webKnossos	2D/webKnossos	Web-based	Knossos	High	-	Python script
<b>FlyEM</b>	2D, 3D/NeuTu	2D/NeuTu	Web-based	DVID	High	-	-
<b>TrackEM2</b>	2D, 3D/TrackEM2	2D/TrackEM2	Web-based	CATMAID	Moderate	-	-
<b>VAST</b>	2D, 3D/VAST	2D/VAST	Central server	VAST	High	-	-
<b>Ilastik</b>	2D, 3D/ Ilastik	2D/ Ilastik	-	HDF5	Low	Random forest	-
<b>Weka</b>	2D/ ImageJ	2D/ ImageJ	-	PNG/TIFF	Low	Random forest	Java script
<b>IMOD</b>	2D/ IMOD	-	-	-	Camera specific	Undefined	-

et al., 2020). One of the tools, NeuroProof (Plaza, 2014), introduces focused and faster proofreading using automated segmentation and prior information (synapse connectivity). Other tools, like Raveler and NeuTu, allow interactive proofreading in a distributed and scalable manner (Farm, 2014; Zhao et al., 2018). Distributed, Versioned, Image-oriented Dataservice (DVID) provides a web-based API for key-value based image labels for efficient storage and faster access. DVID facilitates the distribution and access of data through a common format to access all datasets using a higher-level API (Katz and Plaza, 2019).

Ilastik and Trainable Weka Segmentation (TWS) are plugins in FIJI to segment synaptic junctions and mitochondria (Sommer et al., 2011; Arganda-Carreras et al., 2017). Ilastik originally focused on the work of segmenting synaptic junctions and was further developed into a platform that includes fast interactive training through shallow classifiers (random forests) (Berg et al., 2019). Trainable Weka Segmentation (TWS) allows training of a random forest classifier for binary segmentation and provides options to select the features, load a stored classifier to visualize results on test images along with its performance metrics. Both are extensively used for labeling neuronal 3D images. IMOD can semi-automatically register 3D EM serial sections and was used to segment structures such as small extra-cellular vesicles (Gómez-de Mariscal et al., 2019).

The annotation tools show a trend towards semi-automated segmentation on web frameworks for scalable data access along with providing collaborative proofreading. For further information on accelerating computing and scalable data access for data analysis refer Section 6.



### 4.3. Correlative Light and Electron microscopy (CLEM)

Fluorescence microscopy can help to provide identifying information to EM images and can be used to improve automated analysis. CLEM is used to identify structures targeted with fluorescent probes in  $\mu m$  resolution images at (sub)cellular context from EM (de Boer et al., 2015). Drawitsch et al. (2018) performed CLEM for 40-50 $\mu m$  EM sections for a 3D connectome dataset. The workflow uses the full multi-color space of LM to identify the most-likely axon out of all reconstructed axons in large scale EM to best match with the LM-imaged axonal fluorescent signal. Besides webKnossos, which they used for manual reconstruction of axons that took 5300 work hours for a  $1 \times 1 \times 0.1 \text{ mm}^3$  layer of the mouse neocortex, further speedup using partially automatic methods proposed in (Berning et al., 2015; Dorkenwald et al., 2017; Staffler et al., 2017; Januszewski et al., 2018) is conceivable. Other attempts for 2D CLEM are based on EM workflows or markers to speed up image registration or alignment.

## 5. Segmentation approaches

The taxonomy (Fig. 3 illustrates the main segmentation methodologies reviewed in this section.

### 5.1. Supervised learning

Supervised learning in segmentation refers to the family of machine learning algorithms that use a set of annotated images (training data) to create a computational model that can segment structures in unseen images (test data). The training set is used by the algorithm to determine the model’s parameters in such a way as to maximize the model’s generalization ability.

#### 5.1.1. End-to-end learning

End-to-end learning refers to the use of gradient-based methods to adjust the parameters of a complex deep neural network based on a loss function applied on the network’s prediction (Glasmachers, 2017). In principle, increasing network complexity - e.g. by increasing the number of layers - allows for more complex functions to be learned. In practice, however, there are technical challenges that limit a network’s learning capacity, like vanishing gradients and network degradation (Table 2). The ResNet architecture attempts to counter such limitations with residual blocks (He et al., 2016). Skip connections enable the design of very deep networks while propagating the gradient of the loss function through a lower number of layers. Encoder-decoder architectures, especially U-Nets, have enabled end-to-end learning for segmentation. ResNet blocks have become a standard in encoder and decoder networks for biomedical image segmentation.

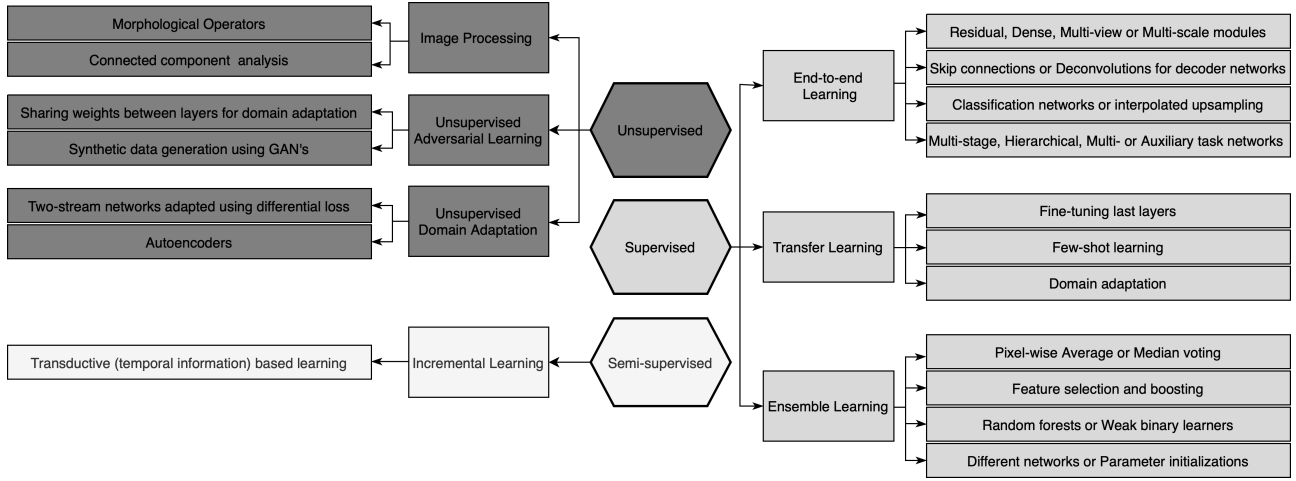


Figure 3: Categorization of deep learning methods used for EM segmentation. Gray shading indicates which components belong to which category (supervised, semi-supervised or unsupervised).

*Neuronal membranes and ResNets.* Various variants of the U-Net architecture using residual blocks have been proposed for segmenting neuronal structures such as membranes, neural cell bodies and cell nucleus. FusionNet and Fully residual CNN (FR-CNN) use residual blocks at each level outperforming the standard U-Net architecture and FCN for membrane segmentation (Quan et al., 2016; He et al., 2020). Dense skip connections that connect each layer to every other layer in a feed-forward manner used in DenseUNets, a combination of U-Net and DenseNet (Cao et al., 2020), achieved competitive segmentation performance on the ISBI 2012 EM dataset. The deconvolutional network of Noh et al. (2015) introduced learnable unpooling layers, was used in combination with residual blocks in the Residual deconvolutional network (RDN) (Fakhry et al., 2016). RDN shows minimal inconsistencies in continuity of membrane detection across the 3D slices on the ISBI 2013 dataset. ResNet with atrous convolutions was used for the segmentation of neural cell bodies and nuclei. Additionally, the multi-scale contextual feature integration outperforms U-Net and Deeplab v3+ (Jiang et al., 2019).

*Mitochondria and efficient 3D networks.* Mitochondrial distribution inside a cell and alterations in its shape are related to degeneration or cellular death. High-resolution automatic analysis is required to study the physiological changes in mitochondria. Both 2D and direct 3D networks for reconstruction work well on isotropic FIB SEM images. A 2D image analysis pipeline for mitochondria segmentation from FIB-SEM dataset was performed by direct upsampling of the encoder features (Oztel et al., 2018). A hybrid 2D-3D network by Xiao et al. (2018) refers to the use of 3D convolutions at the start and end of an encoder-decoder network. Using 2D max-pooling instead of 3D in the same network

helped in capturing anisotropy for SB SEM datasets. Auxiliary supervision in the mid-level features was key for better deep supervision to avoid the vanishing gradient problem. As compared to architectures like U-Net and 3D U-Net, lesser proofreading was needed due to better accuracy.

The 3D networks have millions of parameters to train and are computationally intensive. Multiple views of a 3D stack, three orthogonal views and a final branch to calculate context information from one of the views was used in HIVE-Net, a multi-task pseudo 3D residual network (Yuan et al., 2021). Experiments show that the HIVE-Net with lesser number of parameters achieves state-of-the art performance compared to deep learning models such as U-Net, 3D U-Net or the hybrid 2D-3D network (Xiao et al., 2018).

*Shape-based prior for segmentation.* Shape information is used for faster and regularized segmentation of axons, mitochondria and nuclei to take into account the heterogeneity in large volumes of 3D EM datasets. DeepACSON, a Deep learning-based Automatic Segmentation of axONs, achieves segmentation of lower resolution larger field of view images that miss distinctive image features using shape information (Abdollahzadeh et al., 2021). Faster analysis of low resolution images on par with the high-resolution ones was made possible using shape information, such as ovality of mitochondria, tubularity of axons and circularity of nuclei.

Two-stage networks for shape-based discriminative feature training is performed by using the Hierarchical Encoder Decoder (HED) network (Luo et al., 2021). Based on the eccentricity (elliptic or circular shape) of mitochondria, ground-truth labels are sub-categorized into two sets for training; a first stage multi-task network and a second network for the full labels. Shape information priors used in such networks show less false positives and fewer missed detections in the segmentation of mitochondria when compared with U-Net, 3D U-Net, and HIVE-Net (Yuan et al., 2021).

*Whole cell 3D reconstruction.* Robust and scalable automatic methods for whole-cell 3D reconstruction are required to study intricate organisation of thousands of structures inside a cell. FIB-SEM blocks from 5 different cell types and EM preparation methods were trained for around 35 different cellular organelles. The results show that a diverse set of all samples used for training improves generalizability more than training on only one specific target sample. Such comprehensive datasets and the trained models for 3D reconstruction of cells are made open-source (Heinrich et al., 2021) to allow the exploration of local cellular interactions and their intricate arrangements.

#### 5.1.2. Ensemble learning

Ensemble learning methods combine outputs of multiple predictions for better robustness. Pixel- or voxel-wise averaging and majority or median voting are amongst the main aggregation methods. DeepEM3D uses deep inception-residual modules in the encoding path and multi-scale contextual feature aggregation in the decoding path (Zeng et al., 2017). Variants of the DeepEM3D

architecture use ensemble learning to combine several models that are trained on neuronal boundaries with different thicknesses. Voxel-wise averaging of the predictions account for misalignment and anisotropy in the ssSEM image stacks.

Random forests (Table 2) use ensemble learning for improved generalization. A stack of Random forests was investigated for the segmentation of glomerular basement membrane from TEM images (Cao et al., 2019). Zoom-view random forests based on  $N$  groups of membrane intensity images and one full-view random forest taking  $M$  pixels sampled from all  $N$  groups were trained to capture different imaging conditions. The method of using two-level integrated Random forests enhances generalization on different gray-scale intra-image variations and different morphologies of the membrane. Cetina et al. (2018) used the PIBoost algorithm (Fernández-Baldera and Baumela, 2014), a multi-class generalization of AdaBoost with weak binary learners, for simultaneous segmentation of synapse with mitochondria and mitochondria with membranes. Better accuracy was obtained for both isotropic and anisotropic stacks (SB SEM) due to better representation ability and robustness to class imbalance.

Structured prediction are modelling techniques that forecast a set of values rather than a scalar value. In the segmentation context, structured prediction methods seek the joint prediction of the label of the pixel under consideration as well as the labels of the extended neighbourhood. The hierarchical approach by Peng and Yuan (2019) uses an iterative procedure to fine-tune the segmentation based on handcrafted features preserving neighborhood structure and class labels determined in previous iterations. Structured and cascaded approaches tend to improve the segmentation results by reducing the number of false positives and false negatives.

An ensemble of randomly initialized instances of the same network with each trained on less than 1% of the SB-SEM volume for seven classes in platelet cells yielded the best results to structural variations in large datasets, and outperformed individual 2D and 3D U-Net approaches (Guay et al., 2021a). Multiple network outputs were also combined using a workflow for binary EM segmentation provided by the EM-stellar platform (Khadangi et al., 2021b). The network architectures chosen for experimentation were CDeep3EM, EM-Net, PReLU-Net, ResNet, SegNet, U-Net and VGG-16 (Haberl et al., 2018; Khadangi et al., 2021a; He et al., 2015). A cross-evaluation using a heatmap of different evaluation metrics and networks shows that configuring an ensemble of various architectures is required to obtain the best results. Khadangi et al. (2021b) also demonstrated that no single deep architecture performs consistently well, and that is why ensemble approaches may have an edge over individual methods.

### 5.1.3. Transfer learning

Transfer learning adapts the knowledge acquired from one dataset to another, and is used when an application has insufficient amount of training samples. The pre-trained model is fine-tuned, usually in the final layers, with the training samples of the new dataset. Through transfer learning, the same neural network segmentation pathways have been used across biological systems in 3D (Guay et al., 2019). A three-class segmentation was proposed by Mekuć et al.

(2020) for the delineation of mitochondria, endolysosomes, and background. The domain information of the larger number of mitochondrial structures with texture similar to endolysosomes were used to learn a binary classifier against background. The weights were initialized for training a three-class model where only the last layer was fine-tuned to distinguish between the classes. Transfer learning thus enables the modeling of a dataset even when they are limited.

Fine-tuning a pre-trained network comes with the risk of over-fitting to the few labeled training examples of the new application. This challenge has opened up new research avenues, namely, few-shot learning and domain adaptation. Few-shot is a meta-learning approach that “learns to learn” from a given pre-trained model (Shaban et al., 2017). A pre-trained model is made to learn the similarity or difference between classes on the available few labeled samples, referred to as the support set (Dong and Xing, 2018). Complex non-linear mitochondrial morphology was captured using active feature selection and boosting (Dietlmeier et al., 2019). The VGG-16 model pretrained on the ImageNet dataset was used as a feature extractor for extracting hypercolumns that contain the activations of all CNN layers for each pixel. Hypercolumns were passed through a linear regressor for actively selecting features. Only 20 patches or blocks were used from a FIB-SEM stack for training a gradient based boosting classifier (XGBoost). By actively selecting features and learning using far less training data or even using a single training sample (single-shot) one can obtain competitive segmentation accuracy.

Domain adaptation is another form of transfer learning, where the source to target datasets share the same labels (classes) but have a different data distribution. Changes in data distribution can be due to slightly different experimental parameters during EM imaging or due to the imaging of different tissue types or body locations. Roels et al. (2019) aimed to learn a latent space with a shared encoder in such a way that the source (annotated samples) and target (few annotated samples) representations are aligned in that feature space. Transferring knowledge from isotropic to anisotropic SEM images is possible using learning in latent space for domain adaptation. In contrast, Bermúdez-Chacón et al. (2018) proposed a two networks, jointly trained using a differential loss function to regularize two U-Nets (one for each domain) to avoid domain shift. Only 10% of labeled target data was required for domain adaptation to achieve state-of-the-art performance when compared to a U-Net trained on fully annotated data.

## 5.2. *Semi-supervised learning*

Semi-supervised approaches use unlabeled data for training along with a small set of labeled data (Zhu and Goldberg, 2009). The distribution patterns from unlabeled data used in training models help to generalize more than supervised learning from the few labeled samples. Semi-supervised methods learn to improve the model performance in subsequent iterations using pseudo labels generated from the output of the pre-trained model. Incremental learning selects best features by iteratively adding decision trees to the classifier. (Utgoff,

1989) demonstrated that adding only relevant decision trees can incrementally improve the prediction without needing to go back and retrain the model.

Label propagation in images of a 3D stack using pseudolabels from predictions of a trained network was performed in an incremental setting (Takaya et al., 2021). The experimental results conclude that the generalization performance using supervised learning on 3D EM does not perform well when compared with a sequential semi-supervised segmentation (4S) approach. The 4S approach improved the performance of the network by reducing false positives along with improving segmentation accuracy when compared with U-Net. Such a semi-supervised approach applied on sequential EM images (having strong correlation between images in stacks) reduced the annotation effort by experts.

### 5.3. Unsupervised approaches

Unsupervised approaches are categorized into two groups: the more traditional relies on image processing and thresholding without involving learning algorithms, i.e., by Karabağ et al. (2019) who used traditional image processing algorithms to detect nuclear envelopes. Low-pass filtering, edge detection, dilation to connect disjoint edges, super-pixel analysis followed by smoothing and filling of holes form an unsupervised pipeline for nuclear envelope detection. The pipeline performed better than the four deep learning models VGG16, ResNet18, U-Net and Inception-ResNetv2 investigated by Szegedy et al. (2017). The cell nucleus that becomes smaller at the edges than the middle 2D slices lead to a highly imbalanced images for training the deep architectures. However, the learning-free unsupervised approach assumes that the cell nucleus is always located at the center of the three dimensional stack and that nuclear envelope is darker than nucleus and surrounding background, and therefore such learning-free approaches may not be sufficiently robust in generalization.

The more advanced group of unsupervised approaches configure models from unlabeled data. Unsupervised domain adaptation with self-supervision (self-generated labels) was used to determine pivot locations in the target dataset with no labels that characterise regions of mitochondria or synapse (Bermúdez-Chacón et al., 2019). The target domain locations from the correspondences of similar structures were converted to heatmaps, for adapting the model based on a two-stream U-Net (Bermúdez-Chacón et al., 2018). The results were consistent with those obtained under fully annotated samples trained on U-Net or semi-supervision (use of transfer learning). No new annotation effort in case of domain shifts was required for volumes of FIB-SEM from different mouse specimens.

Adversarial learning trains networks to predict the same output for two datasets, one source and the other being the adversarial perturbed data, for which the latter gives a different output in spite of belonging to the same class. Each algorithm can use a different approach, such as sharing weights across domains (Peng et al., 2020) or use of generative samples from a generator to confuse the discriminator as is done by Generative Adversarial Networks, or GANs for short (Goodfellow et al., 2014). Adversarial learning is also used for domain adaptation to learn non-discriminating features for robustness to shift in

data distributions (Peng et al., 2020). Domain-invariant features in the encoder are learnt through a reconstruction auto-encoder in an unsupervised manner. As the target has no labels, the shared decoder features are still not discriminative to the target domain for which the proposed method uses adversarial learning in the decoder stage. GANs use adversarial learning to generate synthetic training samples with the same statistics as the source training data. Image synthesis using a GAN generates images with similar distribution but varied object configuration for a three-class detection from a TEM dataset (Shaga Devan et al., 2021). Synthetic images speed up automatic image analysis even when large training datasets are not available, thus improving the performance significantly.

#### 5.4. Performance evaluation metrics

Segmentation is evaluated using pixel-based matching or segment-based matching for binary segmentation. When the segmentation gives a unique index to each object it is called instance segmentation, evaluated by penalising overlaps with other individual segments.

Common pixel-based matching measures are accuracy, true positive rates and false positive rates (Jiang et al., 2019). Precision, recall (sensitivity), specificity and F1-score (harmonic mean of precision and recall) are the most basic performance measures used in various studies to quantify the effectiveness of 2D and 3D segmentation methods (Xiao et al., 2018; Dietlmeier et al., 2019; Khadangi et al., 2021b; Takaya et al., 2021). Most binary image segmentation tasks suffer from class imbalance as the background class is much larger than the objects of interest. To address class imbalance, methods such as Intersection over Union (IoU) or Jaccard index, which determine the similarity between the ground-truth and predicted sets, are more appropriate. The Dice similarity coefficient (DSC) addresses class imbalance by only considering the segmentation class for evaluation. The DSC and JAC are the most commonly used measures for performance evaluation in EM (Mekuč et al., 2020; Xiao et al., 2018; Yuan et al., 2021; Luo et al., 2021; Cao et al., 2019; Peng and Yuan, 2019; Bermúdez-Chacón et al., 2018; Peng et al., 2020). The conformity coefficient used by Xiao et al. (2018) is a global similarity score with more discrimination capabilities than Jaccard or DSC (Chang et al., 2009). To calculate how far the segmented structure is from the ground truth, besides the Jaccard index, the Hausdorff distance is another sensible measure (Karabağ et al., 2019). The latter is the spatial distance between two sets, and apart from matching segments, it also takes into account the pixel/voxel localisation. Common metrics used for instance segmentation in (Yuan et al., 2020; Luo et al., 2021) are the Aggregated Jaccard Index (AJI) and the Panoptic Quality (PQ) (Kumar et al., 2017; Kirillov et al., 2019), which account for under- and over-segmentation more accurately than the Jaccard index and DSC. The Jaccard curve, which was inspired by the precision/recall and receiver operating characteristic (ROC) curves, is a measure that quantifies the quality of a segmentation result without involving any thresholds (Cetina et al., 2018). Fig. 4 illustrates how such measures are computed.

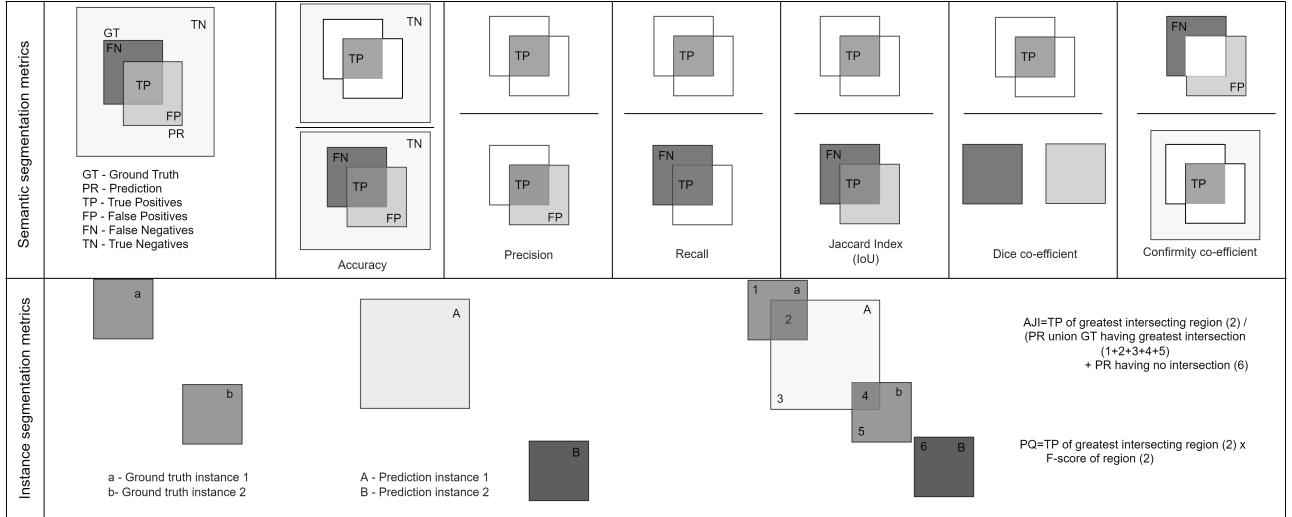


Figure 4: Common performance metrics for binary segmentation. For semantic segmentation, the overall overlap of the ground truth (GT) mask with prediction (PR) is compared without differentiating between objects of the foreground class. For instance segmentation, each GT component is matched with only one PR component, the one with which it has the largest intersection. The PR component *A* overlaps with two GT components, *a* and *b*, but is matched only with *a* due to a larger overlap. The Aggregated Jaccard Index (AJI) takes the sum of the intersections of all matched GT and PR components divided by the sum of their unions plus the unmatched PR components. The Panoptic Quality (PQ) is the sum of the IoU ratios of all associated GT-PR pairs (i.e. TPs) divided by the sum of all TPs and half of the unmatched GT and PR components. The symbol  $|\cdot|$  indicates the area of the component concerned.

Boundary matching and information theoretic scores have emerged as two important metrics to evaluate neuronal boundary maps (Unnikrishnan et al., 2007; Arbelaez et al., 2010; Arganda-Carreras et al., 2015). The most popular ones are similarity-oriented measures between two clusters for paired labels instead of pixel-wise errors. Boundary maps are transformed to segmentations by finding connected components. The rand index quantifies the similarity between the results of two clusters by taking the ratio of the sum of the total number of pairs of points in agreement and pairs of points in disagreements with respect to the total number of pairs between the two clusters. Another measure is based on what are known as the split and merge errors. The split error is computed by taking two randomly selected voxels belonging to the same segment in the ground truth and assessing them based on the joint probability of belonging to the same region in the segmentation result. The merge error is based on whether two voxels predicted as belonging to the same segment do actually belong together. The Rand F-score is then the weighted harmonic mean of the merge and split errors. Metrics like foreground-restricted rand scoring and foreground-restricted information theoretic scoring after border thinning are the state-of-the-art metrics for neuronal boundary segmentation (Cao et al., 2020; Zeng et al., 2017; He et al., 2020; Cetina et al., 2018; Khadangi et al.,



2021b).

## 6. Scalability and performance matters

Bioimage analysis software tools<sup>8</sup> use high-performance computing for scalable processing. Scalability refers to the data processing frameworks and computational resources that can handle big data. Scalable machine or deep learning is not limited by the algorithms involved, but the supporting infrastructure which is vast and complex (Sculley et al., 2015).

### 6.1. Distributed computing

Distributed computing divides a single problem into many parts, controlled by a master node but processed in different computing units (worker nodes). More databases or processing nodes can be added to the system, rather than using a single server with many nodes that is not used at all times. Fault tolerance nodes address hardware failures known as worker nodes or master replica (Fig. 5). Users or clients access and process data remotely in different systems of the network. Biomedical image analysis tools for neuronal reconstruction such as VAST, NeuTu, webKnossos, TrackEM2 (CATMAID) use distributed storage and processing.

Detailed metrics to evaluate for synapse connectivity were introduced in VAST for evaluating petabyte range datasets for 3D EM. A software ecosystem in VAST is used to evaluate two large datasets (Takemura et al., 2015, 2017) deployed in a scalable cluster-based solution using Apache-Spark (Zaharia et al., 2010). The latter is an open source data processing framework to store and process data in batch or real-time across clusters of computers. Distributed Versioned Image-oriented data service (DVID) provides branched or distributed versioning in connectomics reconstruction workflow for collaborating proofreaders from any part of the world (Katz and Plaza, 2019). NeuTu is a client program that uses DVID as its scalable image database for large-scale, collaborative 3D neuronal reconstruction proofreading. A backend Hadoop framework used by Yuan et al. (2020) allows for distributed data storage of large amounts of data. The scaling of clusters with more generated EM data and redundancy of data in various clusters provides reliable data management and integrity.

Decentralized computing, modeled after Google Maps (Rasmussen, 2005), was introduced in the Collaborative Annotation Toolkit for Massive Amounts of Image Data (CATMAID) (Saalfeld et al., 2009). It uses in-browser decentralized annotation of large biological stacks. Immediate or message passing from farther nodes in the network make images accessible to the user (Fig. 5). Projects, image stack information, and annotations (metadata) are stored in a centralized server for cross-referencing and collaboration. WebKnossos uses decentralized systems for image storage of 3D cubes and is implemented for an efficient in-browser access and reconstruction (Boergens et al., 2017).

---

<sup>8</sup><http://www.biii.eu/>

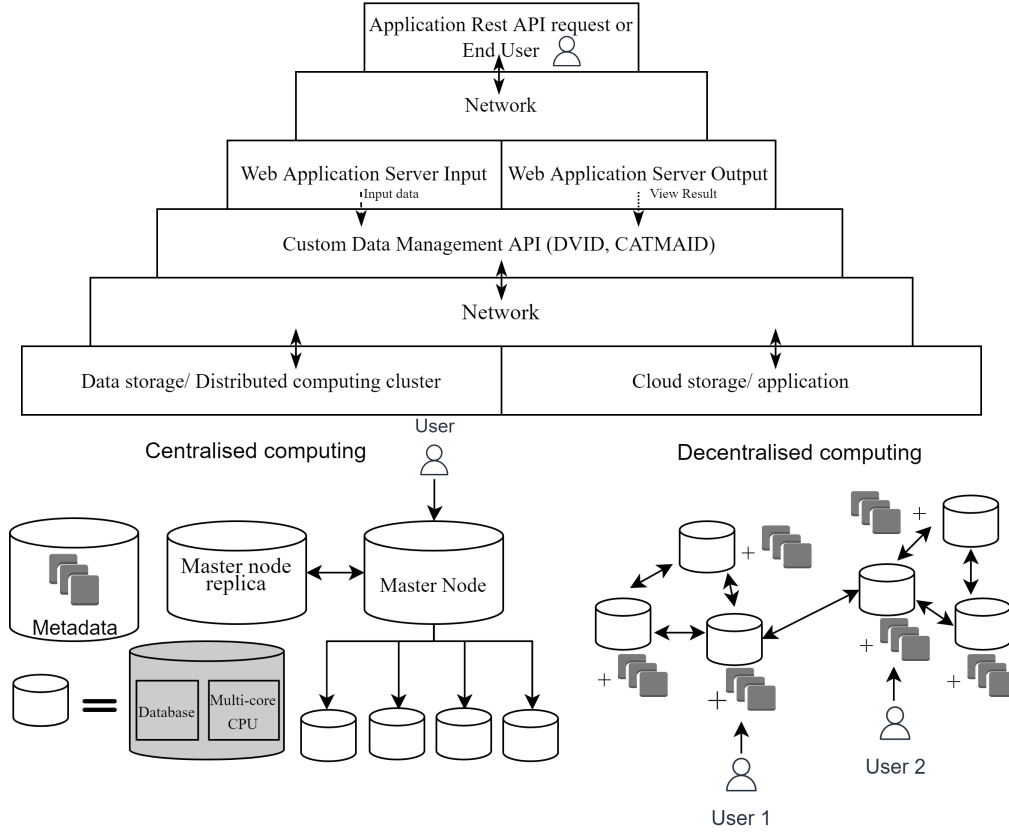


Figure 5: Workflow of bioimage software tools. Data or compute access through web application servers to cluster nodes or cloud entity. An overview of the design for centralised and decentralised computing shows many users accessing concurrently data or compute nodes at the same time in the network.

## 6.2. Cloud computing

Cloud computing is the on-demand provision of servers, applications, networking capabilities, and hardware resources on the internet (Kagadis et al., 2013). There are three models of cloud service. The infrastructure as a service (IaaS) model only includes computing resources, networking, and storage. The platform as a service (PaaS) model includes the application design, testing and development tools, middleware, operating systems, and databases. Finally, the software as a service (SaaS) model facilitates the availability of all application services to users from any device with an internet connection.

CDeep3EM (Haberl et al., 2018), a pre-configured cloud-based implementation of the DeepEM3D CNN for image segmentation, is publicly available on Amazon Web Services (AWS). EM-stellar (Khadangi et al., 2021b) is a Jupyter notebook platform hosted on Google Colab with ready access to cloud computing resources. Colab is a framework for developers to interface with the existing

notebooks and cloud infrastructure to evolve networks for specific microscopy image processing. The aim of the ZeroCostDL4Mic project by von Chamier et al. (2021) is to make deep learning for microscopy analysis accessible to users with no coding experience by leveraging the open, cloud-based Google Colab resources. State-of-the-art networks are provided as notebooks for segmentation, object detection, denoising, and super-resolution microscopy, along with quantitative tools to analyse model performance and optimize it along with data augmentation and transfer learning options.

## 7. Challenges and future trends

CNNs for segmentation are the most popular methods for automatic feature extraction and pixel-wise reconstruction in EM images. A notable example is the U-Net architecture. Techniques for structural segmentation improve robustness through additional supervision or ensemble techniques for detecting less false positives and false negatives. Whole cell 3D reconstruction for segmenting many organelles in volume EM datasets provide public datasets for reuse (Heinrich et al., 2021; Guay et al., 2021a). Large public datasets are not available for training and new datasets generated from EM techniques lack labels for supervised learning. Few-shot learning for segmentation has shown promising results in context of noisy labels and for incremental learning (Dong and Xing, 2018; Liang et al., 2022; Tao et al., 2020). Newer methodologies of semi-supervised and unsupervised learning techniques are becoming more appealing. Semi-supervised and unsupervised methods that can segment new datasets with minimal annotations allow these methods to scale to larger EM datasets. Larger datasets scale well on deeper networks such as transformers that use built-in self-attention between patches which can prove useful for large-scale 2D EM segmentation (Dosovitskiy et al., 2020; Zheng et al., 2021).

Self-supervised methods with the contrastive learning framework have been used to learn similar or dissimilar pairs from data, namely SimCLR (Simple Framework for Contrastive Learning of Visual Representations) and MoCo (Momentum Contrastive Learning) (Chen et al., 2020; Ciga et al., 2020). Networks that are initialized either randomly or by being pretrained on large datasets, such as ImageNet, do not perform better as compared to pre-training using MoCo (Guay et al., 2021b; Casser et al., 2018; Perez et al., 2014; Mekuć et al., 2020). Self-supervised methods can also benefit from multi-modal EM data, such as CLEM. In fact, Seifert et al. (2020) give further insight on the potential of deep learning for automatic image registration for CLEM. Other multi-modal training data that can be used for EM segmentation in the future is ColorEM or EDX information (Pirozzi et al., 2018).

The ability to segment new datasets with minimal annotations allows these methods to scale to larger EM datasets generated from state-of-the-art technologies, such as multi-beam scanning EM. Other aspects of scalability are improving due to the widespread use of distributed or cloud computing. Accessibility by users to such computing resources has also improved through the continued development of bioimage analysis software. Pathologists, for instance, can now

use off-the shelf cloud applications for data access and analysis. Distributed computing can also be performed on the cloud which makes it even more appealing as all required resources can be remotely scaled with ever increasing EM data. Large-scale EM can also benefit more from the Google Maps based decentralized processing approach in a similar manner to improved data access for vEM.

Indexing of segmented structures is important for fast retrieval purposes in practical applications, but it is hardly addressed in this literature. The idea is to enable a domain expert to query a database in three different ways, namely label-based, image-based, and proximity-based. A label-based query would require the user to specify the label of a structure of interest, image-based would require the submission of an image example of a structure of interest and, proximity-based would require the specification of the distance and direction between a set of structures of interest. Such functionality would enable domain experts to enhance their interaction with a database with large volumes of large-scale EM images.

All research data should be Findable, Accessible, Interoperable and reusable (FAIR) for both machine and people (Wilkinson et al., 2016). Findability requires globally identifiable data resource associated with rich metadata, whereas accessibility provides an open, free and universally implementable protocol along with authorization mechanisms for accessing protected data. Interoperability is the data format or knowledge representation language that helps machines understand or be compatible with a service operating on the digital resource. Re-usability requires that an individual or even machine can decide if the resources are useful for any task based on its license terms.

## 8. Conclusion

Automated image analysis techniques for EM are evolving in accordance with the recent advancements in imaging technologies. For instance, automated large-scale 2D EM makes greater demands on the capture of global context by segmentation algorithms, without the aid of 3D information available in volume EM. Given that the lack of fully annotated data in medical imaging will persist and is likely to be compounded by the exponential generation of image data, we suspect that semi-supervised and self-supervised approaches will play a bigger role in the segmentation of EM data in the future.

## 9. Acknowledgement

This project has received funding from the Centre for Data Science and Systems Complexity at the University of Groningen<sup>9</sup>. Part of the work has been sponsored by ZonMW grant 91111.006; the Netherlands Electron Microscopy

---

<sup>9</sup>[www.rug.nl/research/fse/themes/dssc/](http://www.rug.nl/research/fse/themes/dssc/)

Infrastructure (NEMI), NWO National Roadmap for Large-Scale Research Infrastructure of the Dutch Research Council (NWO 184.034.014); the Network for Pancreatic Organ donors with Diabetes (nPOD; RRID:SCR<sub>0</sub>14641), a collaborative T1D research project sponsored by JDRF (nPOD: 5 – *SRA* – 2018 – 557 – *Q* – *R*) and The Leona M. & Harry B. Helmsley Charitable Trust (Grant 2018*PG* – *T1D*053). The content and views expressed are the responsibility of the authors and do not necessarily reflect the official view of nPOD. Organ Procurement Organizations (OPO) partnering with nPOD to provide research resources are listed in <http://www.jdrfnpod.org/for-partners/npod-partners/>.

## References

- Abdollahzadeh, A., Belevich, I., Jokitalo, E., Sierra, A., Tohka, J., 2021. Deepacson automated segmentation of white matter in 3d electron microscopy. *Communications biology* 4, 1–14.
- Arbelaez, P., Maire, M., Fowlkes, C., Malik, J., 2010. Contour detection and hierarchical image segmentation. *IEEE transactions on pattern analysis and machine intelligence* 33, 898–916.
- Arganda-Carreras, I., Kaynig, V., Rueden, C., Eliceiri, K.W., Schindelin, J., Cardona, A., Sebastian Seung, H., 2017. Trainable Weka Segmentation: a machine learning tool for microscopy pixel classification. *Bioinformatics* 33, 2424–2426. doi:10.1093/bioinformatics/btx180.
- Arganda-Carreras, I., Seung, H., Vishwanathan, A., Berger, D., 2013. 3d segmentation of neurites in em images challenge-isbi 2013.
- Arganda-Carreras, I., Turaga, S.C., Berger, D.R., Cireşan, D., Giusti, A., Gambardella, L.M., Schmidhuber, J., Laptev, D., Dwivedi, S., Buhmann, J.M., et al., 2015. Crowdsourcing the creation of image segmentation algorithms for connectomics. *Frontiers in neuroanatomy* , 142.
- Azzopardi, G., Petkov, N., 2012. Trainable cosfire filters for keypoint detection and pattern recognition. *IEEE Transactions on Pattern Analysis and Machine Intelligence* 35, 490 – 503. doi:10.1109/TPAMI.2012.106.
- Badrinarayanan, V., Kendall, A., Cipolla, R., 2017. Segnet: A deep convolutional encoder-decoder architecture for image segmentation. *IEEE transactions on pattern analysis and machine intelligence* 39, 2481–2495.
- Berg, S., Kutra, D., Kroeger, T., Straehle, C.N., Kausler, B.X., Haubold, C., Schiegg, M., Ales, J., Beier, T., Rudy, M., et al., 2019. Ilastik: interactive machine learning for (bio) image analysis. *Nature Methods* 16, 1226–1232.
- Berger, D.R., Seung, H.S., Lichtman, J.W., 2018. Vast (volume annotation and segmentation tool): efficient manual and semi-automatic labeling of large 3d image stacks. *Frontiers in neural circuits* 12, 88.

- Bermúdez-Chacón, R., Altingövdé, O., Becker, C., Salzmänn, M., Fua, P., 2019. Visual correspondences for unsupervised domain adaptation on electron microscopy images. *IEEE transactions on medical imaging* 39, 1256–1267.
- Bermúdez-Chacón, R., Márquez-Neila, P., Salzmänn, M., Fua, P., 2018. A domain-adaptive two-stream u-net for electron microscopy image segmentation, in: 2018 IEEE 15th International Symposium on Biomedical Imaging (ISBI 2018), IEEE. pp. 400–404.
- Berning, M., Boergens, K.M., Helmstaedter, M., 2015. Segem: efficient image analysis for high-resolution connectomics. *Neuron* 87, 1193–1206.
- de Boer, P., Giepmans, B.N., 2021. State-of-the-art microscopy to understand islets of langerhans: what to expect next? *Immunology and Cell Biology* 99, 509–520.
- de Boer, P., Hoogenboom, J., Giepmans, B., 2015. Correlated light and electron microscopy: ultrastructure lights up! *Nature Methods* 12, 503–513.
- de Boer, P., Pirozzi, N.M., Wolters, A.H., Kuipers, J., Kusmartseva, I., Atkinson, M.A., Campbell-Thompson, M., Giepmans, B.N., 2020. Large-scale electron microscopy database for human type 1 diabetes. *Nature communications* 11, 1–9.
- Boergens, K.M., Berning, M., Bocklisch, T., Bräunlein, D., Drawitsch, F., Frohnhofen, J., Herold, T., Otto, P., Rzepka, N., Werkmeister, T., et al., 2017. webknossos: efficient online 3d data annotation for connectomics. *nature methods* 14, 691–694.
- Boser, B.E., Guyon, I.M., Vapnik, V.N., 1992. A training algorithm for optimal margin classifiers, in: *Proceedings of the fifth annual workshop on Computational learning theory*, pp. 144–152.
- Breiman, L., 2001. Random forests. *Machine learning* 45, 5–32.
- Cao, L., Lu, Y., Li, C., Yang, W., 2019. Automatic segmentation of pathological glomerular basement membrane in transmission electron microscopy images with random forest stacks. *Computational and mathematical methods in medicine* 2019.
- Cao, Y., Liu, S., Peng, Y., Li, J., 2020. Denseunet: densely connected unet for electron microscopy image segmentation. *IET Image Processing* 14, 2682–2689.
- Casser, V., Kang, K., Pfister, H., Haehn, D., 2018. Fast mitochondria segmentation for connectomics. *arXiv preprint arXiv:1812.06024* .
- Cetina, K., Buenaposada, J.M., Baumela, L., 2018. Multi-class segmentation of neuronal structures in electron microscopy images. *BMC bioinformatics* 19, 1–13.

- von Chamier, L., Laine, R.F., Jukkala, J., Spahn, C., Krentzel, D., Nehme, E., Lerche, M., Hernández-Pérez, S., Mattila, P.K., Karinou, E., et al., 2021. Democratising deep learning for microscopy with zerocostdl4mic. *Nature communications* 12, 1–18.
- Chang, H.H., Zhuang, A.H., Valentino, D.J., Chu, W.C., 2009. Performance measure characterization for evaluating neuroimage segmentation algorithms. *Neuroimage* 47, 122–135.
- Chen, L.C., Papandreou, G., Kokkinos, I., Murphy, K., Yuille, A.L., 2014. Semantic image segmentation with deep convolutional nets and fully connected crfs. *arXiv preprint arXiv:1412.7062* .
- Chen, L.C., Papandreou, G., Kokkinos, I., Murphy, K., Yuille, A.L., 2017a. Deeplab: Semantic image segmentation with deep convolutional nets, atrous convolution, and fully connected crfs. *IEEE transactions on pattern analysis and machine intelligence* 40, 834–848.
- Chen, L.C., Papandreou, G., Schroff, F., Adam, H., 2017b. Rethinking atrous convolution for semantic image segmentation. *arXiv preprint arXiv:1706.05587* .
- Chen, L.C., Zhu, Y., Papandreou, G., Schroff, F., Adam, H., 2018. Encoder-decoder with atrous separable convolution for semantic image segmentation, in: *Proceedings of the European conference on computer vision (ECCV)*, pp. 801–818.
- Chen, T., Kornblith, S., Norouzi, M., Hinton, G., 2020. A simple framework for contrastive learning of visual representations, in: *International conference on machine learning*, PMLR. pp. 1597–1607.
- Ciga, O., Martel, A.L., Xu, T., 2020. Self supervised contrastive learning for digital histopathology. *arXiv preprint arXiv:2011.13971* .
- Ciresan, D., Giusti, A., Gambardella, L., Schmidhuber, J., 2012. Deep neural networks segment neuronal membranes in electron microscopy images. *Advances in neural information processing systems* 25, 2843–2851.
- Dalal, N., Triggs, B., 2005. Histograms of oriented gradients for human detection, in: *2005 IEEE computer society conference on computer vision and pattern recognition (CVPR'05)*, Ieee. pp. 886–893.
- Dietlmeier, J., McGuinness, K., Rugonyi, S., Wilson, T., Nuttall, A., O'Connor, N.E., 2019. Few-shot hypercolumn-based mitochondria segmentation in cardiac and outer hair cells in focused ion beam-scanning electron microscopy (fib-sem) data. *Pattern recognition letters* 128, 521–528.
- Dittmayer, C., Goebel, H.H., Heppner, F.L., Stenzel, W., Bachmann, S., 2021. Preparation of samples for large-scale automated electron microscopy of tissue and cell ultrastructure. *Microscopy and Microanalysis* 27, 815–827.

- Dong, N., Xing, E.P., 2018. Few-shot semantic segmentation with prototype learning., in: BMVC.
- Dorkenwald, S., Schubert, P.J., Killinger, M.F., Urban, G., Mikula, S., Svara, F., Kornfeld, J., 2017. Automated synaptic connectivity inference for volume electron microscopy. *Nature methods* 14, 435–442.
- Dosovitskiy, A., Beyer, L., Kolesnikov, A., Weissenborn, D., Zhai, X., Unterthiner, T., Dehghani, M., Minderer, M., Heigold, G., Gelly, S., et al., 2020. An image is worth 16x16 words: Transformers for image recognition at scale. *arXiv preprint arXiv:2010.11929* .
- Drawitsch, F., Karimi, A., Boergens, K.M., Helmstaedter, M., 2018. Fluorimetry, virtual labeling of axons in three-dimensional electron microscopy data for long-range connectomics. *Elife* 7, e38976.
- Dreiseitl, S., Ohno-Machado, L., 2002. Logistic regression and artificial neural network classification models: a methodology review. *Journal of biomedical informatics* 35, 352–359.
- Drucker, H., Cortes, C., 1995. Boosting decision trees. *Advances in neural information processing systems* 8.
- Eberle, A., Mikula, S., Schalek, R., Lichtman, J., Tate, M.K., Zeidler, D., 2015. High-resolution, high-throughput imaging with a multibeam scanning electron microscope. *Journal of microscopy* 259, 114–120.
- Faas, F.G., Avramut, M.C., M. van den Berg, B., Mommaas, A.M., Koster, A.J., Ravelli, R.B., 2012. Virtual nanoscopy: generation of ultra-large high resolution electron microscopy maps. *Journal of Cell Biology* 198, 457–469.
- Fakhry, A., Zeng, T., Ji, S., 2016. Residual deconvolutional networks for brain electron microscopy image segmentation. *IEEE transactions on medical imaging* 36, 447–456.
- Farm, J., 2014. Raveler.
- Fernández-Baldera, A., Baumela, L., 2014. Multi-class boosting with asymmetric binary weak-learners. *Pattern Recognition* 47, 2080–2090.
- Gecer, B., Azzopardi, G., Petkov, N., 2017. Color-blob-based cosfire filters for object recognition. *Image and Vision Computing* 57, 165–174. doi:<https://doi.org/10.1016/j.imavis.2016.10.006>.
- Glasmachers, T., 2017. Limits of end-to-end learning, in: *Asian Conference on Machine Learning*, PMLR. pp. 17–32.
- Glorot, X., Bengio, Y., 2010. Understanding the difficulty of training deep feedforward neural networks, in: *Proceedings of the thirteenth international conference on artificial intelligence and statistics, JMLR Workshop and Conference Proceedings*. pp. 249–256.



- Goodfellow, I., Pouget-Abadie, J., Mirza, M., Xu, B., Warde-Farley, D., Ozair, S., Courville, A., Bengio, Y., 2014. Generative adversarial nets. *Advances in neural information processing systems* 27.
- Guay, M.D., Emam, Z.A., Anderson, A.B., Aronova, M.A., Pokrovskaya, I.D., Storrie, B., Leapman, R.D., 2021a. Dense cellular segmentation for em using 2d–3d neural network ensembles. *Scientific reports* 11, 1–11.
- Guay, M.D., Emam, Z.A., Anderson, A.B., Aronova, M.A., Pokrovskaya, I.D., Storrie, B., Leapman, R.D., 2021b. Dense cellular segmentation for em using 2d–3d neural network ensembles. *Scientific reports* 11, 1–11.
- Guay, M.D., Emam, Z.A., Anderson, A.B., Leapman, R.D., 2019. Transfer learning for efficient segmentation of subcellular structures in 3-d electron microscopy. *Biophysical Journal* 116, 288a.
- Haberl, M.G., Churas, C., Tindall, L., Boassa, D., Phan, S., Bushong, E.A., Madany, M., Akay, R., Deerinck, T.J., Peltier, S.T., et al., 2018. Cdeep3m—plug-and-play cloud-based deep learning for image segmentation. *Nature methods* 15, 677–680.
- Haehn, D., Knowles-Barley, S., Roberts, M., Beyer, J., Kasthuri, N., Lichtman, J.W., Pfister, H., 2014. Design and evaluation of interactive proofreading tools for connectomics. *IEEE transactions on visualization and computer graphics* 20, 2466–2475.
- He, J., Xiang, S., Zhu, Z., 2020. A deep fully residual convolutional neural network for segmentation in em images. *International Journal of Wavelets, Multiresolution and Information Processing* 18, 2050007.
- He, K., Zhang, X., Ren, S., Sun, J., 2015. Delving deep into rectifiers: Surpassing human-level performance on imagenet classification, in: *Proceedings of the IEEE international conference on computer vision*, pp. 1026–1034.
- He, K., Zhang, X., Ren, S., Sun, J., 2016. Deep residual learning for image recognition, in: *Proceedings of the IEEE conference on computer vision and pattern recognition*, pp. 770–778.
- Heinrich, L., Bennett, D., Ackerman, D., Park, W., Bogovic, J., Eckstein, N., Petruncio, A., Clements, J., Pang, S., Xu, C.S., et al., 2021. Whole-cell organelle segmentation in volume electron microscopy. *Nature* , 1–6.
- Helmstaedter, M., Briggman, K.L., Denk, W., 2011. High-accuracy neurite reconstruction for high-throughput neuroanatomy. *Nature neuroscience* 14, 1081–1088.
- Hochreiter, S., Schmidhuber, J., 1997. Long short-term memory. *Neural computation* 9, 1735–1780.

- Huang, G., Liu, Z., Van Der Maaten, L., Weinberger, K.Q., 2017. Densely connected convolutional networks, in: *Proceedings of the IEEE conference on computer vision and pattern recognition*, pp. 4700–4708.
- Iudin, A., Korir, P.K., Salavert-Torres, J., Kleywegt, G.J., Patwardhan, A., 2016. Empiar: a public archive for raw electron microscopy image data. *Nature methods* 13, 387–388.
- Januszewski, M., Kornfeld, J., Li, P.H., Pope, A., Blakely, T., Lindsey, L., Maitin-Shepard, J., Tyka, M., Denk, W., Jain, V., 2018. High-precision automated reconstruction of neurons with flood-filling networks. *Nature methods* 15, 605–610.
- Jiang, Y., Xiao, C., Li, L., Chen, X., Shen, L., Han, H., 2019. An effective encoder-decoder network for neural cell bodies and cell nucleus segmentation of em images, in: *2019 41st Annual International Conference of the IEEE Engineering in Medicine and Biology Society (EMBC)*, IEEE. pp. 6302–6305.
- Kagadis, G.C., Kloukinas, C., Moore, K., Philbin, J., Papadimitroulas, P., Alexakos, C., Nagy, P.G., Visvikis, D., Hendee, W.R., 2013. Cloud computing in medical imaging. *Medical physics* 40, 070901.
- Karabağ, C., Jones, M.L., Peddie, C.J., Weston, A.E., Collinson, L.M., Reyes-Aldasoro, C.C., 2019. Segmentation and modelling of the nuclear envelope of hela cells imaged with serial block face scanning electron microscopy. *Journal of Imaging* 5, 75.
- Kasthuri, N., Hayworth, K.J., Berger, D.R., Schalek, R.L., Conchello, J.A., Knowles-Barley, S., Lee, D., Vázquez-Reina, A., Kaynig, V., Jones, T.R., et al., 2015. Saturated reconstruction of a volume of neocortex. *Cell* 162, 648–661.
- Katz, W.T., Plaza, S.M., 2019. Dvid: distributed versioned image-oriented dataservice. *Frontiers in neural circuits* 13, 5.
- Khadangi, A., Boudier, T., Rajagopal, V., 2021a. Em-net: Deep learning for electron microscopy image segmentation, in: *2020 25th International Conference on Pattern Recognition (ICPR)*, IEEE. pp. 31–38.
- Khadangi, A., Boudier, T., Rajagopal, V., 2021b. Em-stellar: benchmarking deep learning for electron microscopy image segmentation. *Bioinformatics* 37, 97–106.
- Kirillov, A., He, K., Girshick, R., Rother, C., Dollár, P., 2019. Panoptic segmentation, in: *Proceedings of the IEEE/CVF Conference on Computer Vision and Pattern Recognition*, pp. 9404–9413.
- Krizhevsky, A., Sutskever, I., Hinton, G.E., 2012. Imagenet classification with deep convolutional neural networks. *Advances in neural information processing systems* 25, 1097–1105.

- Kucukelbir, A., Sigworth, F.J., Tagare, H.D., 2014. Quantifying the local resolution of cryo-em density maps. *Nature methods* 11, 63–65.
- Kumar, N., Verma, R., Sharma, S., Bhargava, S., Vahadane, A., Sethi, A., 2017. A dataset and a technique for generalized nuclear segmentation for computational pathology. *IEEE transactions on medical imaging* 36, 1550–1560.
- LeCun, Y., Bengio, Y., Hinton, G., 2015. Deep learning. *nature* 521, 436–444.
- Li, W., Liu, J., Xiao, C., Deng, H., Xie, Q., Han, H., 2018. A fast forward 3d connection algorithm for mitochondria and synapse segmentations from serial em images. *BioData mining* 11, 1–15.
- Liang, K.J., Rangrej, S.B., Petrovic, V., Hassner, T., 2022. Few-shot learning with noisy labels. *arXiv preprint arXiv:2204.05494* .
- Long, J., Shelhamer, E., Darrell, T., 2015. Fully convolutional networks for semantic segmentation, in: *Proceedings of the IEEE conference on computer vision and pattern recognition*, pp. 3431–3440.
- Lowe, D.G., 2004. Distinctive image features from scale-invariant keypoints. *International journal of computer vision* 60, 91–110.
- Lucchi, A., Li, Y., Fua, P., 2013. Learning for structured prediction using approximate subgradient descent with working sets, in: *Proceedings of the IEEE Conference on Computer Vision and Pattern Recognition*, pp. 1987–1994.
- Luo, Z., Wang, Y., Liu, S., Peng, J., 2021. Hierarchical encoder-decoder with soft label-decomposition for mitochondria segmentation in em images. *Frontiers in Neuroscience* 15.
- Mané, D., et al., 2015. Tensorboard: Tensorflow’s visualization toolkit. Retrieved October 8, 2021.
- Gómez-de Mariscal, E., Maška, M., Kotrbová, A., Pospíchalová, V., Matula, P., Muñoz-Barrutia, A., 2019. Deep-learning-based segmentation of small extracellular vesicles in transmission electron microscopy images. *Scientific reports* 9, 1–10.
- Masci, J., Meier, U., Cireşan, D., Schmidhuber, J., 2011. Stacked convolutional auto-encoders for hierarchical feature extraction, in: *International conference on artificial neural networks*, Springer. pp. 52–59.
- Mekuč, M.Ž., Bohak, C., Hudoklin, S., Kim, B.H., Kim, M.Y., Marolt, M., et al., 2020. Automatic segmentation of mitochondria and endolysosomes in volumetric electron microscopy data. *Computers in biology and medicine* 119, 103693.

- Motta, A., Berning, M., Boergens, K.M., Staffler, B., Beining, M., Loomba, S., Hennig, P., Wissler, H., Helmstaedter, M., 2019. Dense connectomic reconstruction in layer 4 of the somatosensory cortex. *Science* 366.
- Noh, H., Hong, S., Han, B., 2015. Learning deconvolution network for semantic segmentation, in: *Proceedings of the IEEE international conference on computer vision*, pp. 1520–1528.
- Oktay, O., Schlemper, J., Folgoc, L.L., Lee, M., Heinrich, M., Misawa, K., Mori, K., McDonagh, S., Hammerla, N.Y., Kainz, B., et al., 2018. Attention u-net: Learning where to look for the pancreas. *arXiv preprint arXiv:1804.03999* .
- Oztel, I., Yolcu, G., Ersoy, I., White, T.A., Bunyak, F., 2018. Deep learning approaches in electron microscopy imaging for mitochondria segmentation. *International Journal of Data Mining and Bioinformatics* 21, 91–106.
- Peddie, C.J., Collinson, L.M., 2014. Exploring the third dimension: volume electron microscopy comes of age. *Micron* 61, 9–19.
- Peddie, C.J., Genoud, C., Kreshuk, A., Meechan, K., Micheva, K.D., Narayan, K., Pape, C., Parton, R.G., Schieber, N.L., Schwab, Y., et al., 2022. Volume electron microscopy. *Nature Reviews Methods Primers* 2, 1–23.
- Peng, J., Yi, J., Yuan, Z., 2020. Unsupervised mitochondria segmentation in em images via domain adaptive multi-task learning. *IEEE Journal of Selected Topics in Signal Processing* 14, 1199–1209.
- Peng, J., Yuan, Z., 2019. Mitochondria segmentation from em images via hierarchical structured contextual forest. *IEEE journal of biomedical and health informatics* 24, 2251–2259.
- Perez, A.J., Seyedhosseini, M., Deerinck, T.J., Bushong, E.A., Panda, S., Tasdizen, T., Ellisman, M.H., 2014. A workflow for the automatic segmentation of organelles in electron microscopy image stacks. *Frontiers in neuroanatomy* 8, 126.
- Pirozzi, N.M., Hoogenboom, J.P., Giepmans, B.N., 2018. Colorem: analytical electron microscopy for element-guided identification and imaging of the building blocks of life. *Histochemistry and cell biology* 150, 509–520.
- Plaza, S.M., 2014. Focused proofreading: efficiently extracting connectomes from segmented em images. *arXiv preprint arXiv:1409.1199* .
- Plaza, S.M., Funke, J., 2018. Analyzing image segmentation for connectomics. *Frontiers in neural circuits* 12, 102.
- Quan, T.M., Hildebrand, D.G., Jeong, W.K., 2016. Fusionnet: A deep fully residual convolutional neural network for image segmentation in connectomics.

- Rasmussen, L., 2005. Keynote: google maps and browser support for rich web applications. *Lecture Notes in Computer Science* 3579, 7.
- Ravelli, R.B., Kalicharan, R.D., Avramut, M.C., Sjollem, K.A., Pronk, J.W., Dijk, F., Koster, A.J., Visser, J.T., Faas, F.G., Giepmans, B.N., 2013. Destruction of tissue, cells and organelles in type 1 diabetic rats presented at macromolecular resolution. *Scientific reports* 3, 1–6.
- Ren, Y., Kruit, P., 2016. Transmission electron imaging in the delft multibeam scanning electron microscope 1. *Journal of Vacuum Science & Technology B, Nanotechnology and Microelectronics: Materials, Processing, Measurement, and Phenomena* 34, 06KF02.
- Roels, J., Hennies, J., Saeys, Y., Philips, W., Kreshuk, A., 2019. Domain adaptive segmentation in volume electron microscopy imaging, in: 2019 IEEE 16th International Symposium on Biomedical Imaging (ISBI 2019), IEEE. pp. 1519–1522.
- Ronneberger, O., Fischer, P., Brox, T., 2015. U-net: Convolutional networks for biomedical image segmentation, in: *International Conference on Medical image computing and computer-assisted intervention*, Springer. pp. 234–241.
- Saalfeld, S., Cardona, A., Hartenstein, V., Tomančák, P., 2009. Catmaid: collaborative annotation toolkit for massive amounts of image data. *Bioinformatics* 25, 1984–1986.
- Scheffer, L.K., Xu, C.S., Januszewski, M., Lu, Z., Takemura, S.y., Hayworth, K.J., Huang, G.B., Shinomiya, K., Maitlin-Shepard, J., Berg, S., et al., 2020. A connectome and analysis of the adult drosophila central brain. *Elife* 9.
- Sculley, D., Holt, G., Golovin, D., Davydov, E., Phillips, T., Ebner, D., Chaudhary, V., Young, M., Crespo, J.F., Dennison, D., 2015. Hidden technical debt in machine learning systems. *Advances in neural information processing systems* 28.
- Seifert, R., Markert, S.M., Britz, S., Perschin, V., Erbacher, C., Stigloher, C., Kollmannsberger, P., 2020. Deepclem: automated registration for correlative light and electron microscopy using deep learning. *F1000Research* 9, 1275.
- Shaban, A., Bansal, S., Liu, Z., Essa, I., Boots, B., 2017. One-shot learning for semantic segmentation. *arXiv preprint arXiv:1709.03410* .
- Shaga Devan, K., Walther, P., von Einem, J., Ropinski, T., A Kestler, H., Read, C., 2021. Improved automatic detection of herpesvirus secondary envelopment stages in electron microscopy by augmenting training data with synthetic labelled images generated by a generative adversarial network. *Cellular Microbiology* 23, e13280.
- Simonyan, K., Zisserman, A., 2014. Very deep convolutional networks for large-scale image recognition. *arXiv preprint arXiv:1409.1556* .

- Sokol, E., Kramer, D., Diercks, G.F., Kuipers, J., Jonkman, M.F., Pas, H.H., Giepmans, B.N., 2015. Large-scale electron microscopy maps of patient skin and mucosa provide insight into pathogenesis of blistering diseases. *Journal of Investigative Dermatology* 135, 1763–1770.
- Sommer, C., Straehle, C., Koethe, U., Hamprecht, F.A., 2011. Ilastik: Interactive learning and segmentation toolkit, in: 2011 IEEE international symposium on biomedical imaging: From nano to macro, IEEE. pp. 230–233.
- Spiers, H., Songhurst, H., Nightingale, L., de Folter, J., Community, Z.V., Hutchings, R., Peddie, C.J., Weston, A., Strange, A., Hindmarsh, S., et al., 2021. Deep learning for automatic segmentation of the nuclear envelope in electron microscopy data, trained with volunteer segmentations. *Traffic* .
- Srivastava, R.K., Greff, K., Schmidhuber, J., 2015. Highway networks. *arXiv preprint arXiv:1505.00387* .
- Staffler, B., Berning, M., Boergens, K.M., Gour, A., van der Smagt, P., Helmstaedter, M., 2017. Synem, automated synapse detection for connectomics. *Elife* 6, e26414.
- Szegedy, C., Ioffe, S., Vanhoucke, V., Alemi, A.A., 2017. Inception-v4, inception-resnet and the impact of residual connections on learning, in: Thirty-first AAAI conference on artificial intelligence.
- Szegedy, C., Liu, W., Jia, Y., Sermanet, P., Reed, S., Anguelov, D., Erhan, D., Vanhoucke, V., Rabinovich, A., 2015. Going deeper with convolutions, in: Proceedings of the IEEE conference on computer vision and pattern recognition, pp. 1–9.
- Takaya, E., Takeichi, Y., Ozaki, M., Kurihara, S., 2021. Sequential semi-supervised segmentation for serial electron microscopy image with small number of labels. *Journal of Neuroscience Methods* 351, 109066.
- Takemura, S.y., Aso, Y., Hige, T., Wong, A., Lu, Z., Xu, C.S., Rivlin, P.K., Hess, H., Zhao, T., Parag, T., et al., 2017. A connectome of a learning and memory center in the adult drosophila brain. *Elife* 6, e26975.
- Takemura, S.y., Xu, C.S., Lu, Z., Rivlin, P.K., Parag, T., Olbris, D.J., Plaza, S., Zhao, T., Katz, W.T., Umayam, L., et al., 2015. Synaptic circuits and their variations within different columns in the visual system of drosophila. *Proceedings of the National Academy of Sciences* 112, 13711–13716.
- Tao, X., Hong, X., Chang, X., Dong, S., Wei, X., Gong, Y., 2020. Few-shot class-incremental learning, in: Proceedings of the IEEE/CVF Conference on Computer Vision and Pattern Recognition, pp. 12183–12192.
- Titze, B., Genoud, C., 2016. Volume scanning electron microscopy for imaging biological ultrastructure. *Biology of the Cell* 108, 307–323.

- Unnikrishnan, R., Pantofaru, C., Hebert, M., 2007. Toward objective evaluation of image segmentation algorithms. *IEEE transactions on pattern analysis and machine intelligence* 29, 929–944.
- Urakubo, H., Bullmann, T., Kubota, Y., Oba, S., Ishii, S., 2019. Uni-em: An environment for deep neural network-based automated segmentation of neuronal electron microscopic images. *Scientific reports* 9, 1–9.
- Utgoff, P.E., 1989. Incremental induction of decision trees. *Machine learning* 4, 161–186.
- Wang, L., He, D.C., 1990. Texture classification using texture spectrum. *Pattern recognition* 23, 905–910.
- Wilkinson, M.D., Dumontier, M., Aalbersberg, I.J., Appleton, G., Axton, M., Baak, A., Blomberg, N., Boiten, J.W., da Silva Santos, L.B., Bourne, P.E., et al., 2016. The fair guiding principles for scientific data management and stewardship. *Scientific data* 3, 1–9.
- Xiao, C., Chen, X., Li, W., Li, L., Wang, L., Xie, Q., Han, H., 2018. Automatic mitochondria segmentation for em data using a 3d supervised convolutional network. *Frontiers in neuroanatomy* 12, 92.
- Yamashita, R., Nishio, M., Do, R.K.G., Togashi, K., 2018. Convolutional neural networks: an overview and application in radiology. *Insights into imaging* 9, 611–629.
- Yuan, J., Zhang, J., Shen, L., Zhang, D., Yu, W., Han, H., 2020. Massive data management and sharing module for connectome reconstruction. *Brain Sciences* 10, 314.
- Yuan, Z., Ma, X., Yi, J., Luo, Z., Peng, J., 2021. Hive-net: Centerline-aware hierarchical view-ensemble convolutional network for mitochondria segmentation in em images. *Computer Methods and Programs in Biomedicine* 200, 105925.
- Zaharia, M., Chowdhury, M., Franklin, M.J., Shenker, S., Stoica, I., 2010. Spark: Cluster computing with working sets, in: 2nd USENIX Workshop on Hot Topics in Cloud Computing (HotCloud 10).
- Zeng, T., Wu, B., Ji, S., 2017. Deepem3d: approaching human-level performance on 3d anisotropic em image segmentation. *Bioinformatics* 33, 2555–2562.
- Zhao, H., Shi, J., Qi, X., Wang, X., Jia, J., 2017. Pyramid scene parsing network, in: *Proceedings of the IEEE conference on computer vision and pattern recognition*, pp. 2881–2890.
- Zhao, T., Olbris, D.J., Yu, Y., Plaza, S.M., 2018. Neutu: software for collaborative, large-scale, segmentation-based connectome reconstruction. *Frontiers in Neural Circuits* 12, 101.

- Zheng, S., Lu, J., Zhao, H., Zhu, X., Luo, Z., Wang, Y., Fu, Y., Feng, J., Xiang, T., Torr, P.H., et al., 2021. Rethinking semantic segmentation from a sequence-to-sequence perspective with transformers, in: Proceedings of the IEEE/CVF conference on computer vision and pattern recognition, pp. 6881–6890.
- Zhu, X., Goldberg, A.B., 2009. Introduction to semi-supervised learning. Synthesis lectures on artificial intelligence and machine learning 3, 1–130.